

RSC Advances



This is an *Accepted Manuscript*, which has been through the Royal Society of Chemistry peer review process and has been accepted for publication.

Accepted Manuscripts are published online shortly after acceptance, before technical editing, formatting and proof reading. Using this free service, authors can make their results available to the community, in citable form, before we publish the edited article. This *Accepted Manuscript* will be replaced by the edited, formatted and paginated article as soon as this is available.

You can find more information about *Accepted Manuscripts* in the [Information for Authors](#).

Please note that technical editing may introduce minor changes to the text and/or graphics, which may alter content. The journal's standard [Terms & Conditions](#) and the [Ethical guidelines](#) still apply. In no event shall the Royal Society of Chemistry be held responsible for any errors or omissions in this *Accepted Manuscript* or any consequences arising from the use of any information it contains.

Sol-gel synthesis and room-temperature properties of α -LiZr₂(PO₄)₃

Hany El-Shinawi,^{a,c*} Colin Greaves,^b Jürgen Janek^a

^a Institute of Physical Chemistry, Justus-Liebig-University, Heinrich-Buff-Ring 58, 35392 Giessen, Germany.

^b School of Chemistry, University of Birmingham, Birmingham B15 2TT, UK

^c Permanent address: Chemistry department, Faculty of Science, Mansoura University, Mansoura 35516, Egypt.

Corresponding Author

*Dr. Hany El-Shinawi

Institute of Physical Chemistry, Justus-Liebig-University, Giessen

Heinrich-Buff-Ring 58, 35392 Giessen, Germany

Tel.: (+49641) 99-34514, Fax: (+49641) 99-34509

H_elshinawi@mans.edu.eg

ABSTRACT

The structural and electrical properties of α -LiZr₂(PO₄)₃ are studied at room temperature for the first time. A room-temperature stable α -LiZr₂(PO₄)₃ phase ($R\bar{3}c$, $a = 8.85196(4)$ Å and $c = 22.1510(1)$ Å) is prepared by a modified sol-gel approach. The material exhibits a room-temperature (25 °C) total conductivity of 1.63×10^{-6} Scm⁻¹ at a density of 76 % of the theoretical density. A room-temperature bulk conductivity as high as 1.58×10^{-4} Scm⁻¹ can be estimated from the impedance measurements. Conductivity measurements suggest that a nominal $\alpha \rightarrow \alpha'$ phase transition occurs below room-temperature (at about 16–18 °C). The activation energies for the conductivity of the α and α' phases are 0.39 and 0.99 eV, respectively (in the temperature range –20 – 100 °C).

KEYWORDS: Lithium zirconium phosphate, phase transition, NASICON, solid electrolyte

1. INTRODUCTION

Lithium ion conducting NASICONs are widely investigated as potential solid electrolytes for lithium battery applications. NASICON-structured $\text{Li}_x\text{B}_2(\text{PO}_4)_3$ phases exhibit a framework structure consisting of corner-shared PO_4 tetrahedra and BO_6 octahedra, which can accommodate lithium ions in two types of interstitial sites, commonly referred to as M1 and M2; the M1 sites are situated between pairs of BO_6 octahedra along the c-axis, while the M2 sites are located between infinite ribbons of $[\text{O}_3\text{BO}_3\text{M1O}_3\text{BO}_3\cdots\text{O}_3\text{BO}_3\text{M1}]_\infty$ (Figure 1). $\text{LiB}_2(\text{PO}_4)_3$ NASICONs ideally crystallize in the rhombohedral $R\bar{3}c$ space group where lithium selectively occupies the M1 sites. Among the different Li^+ conducting NASICONs, titanium-based ones exhibit the highest lithium ion conductivity at room temperature (up to $3 \times 10^{-3} \text{ Scm}^{-1}$ for $\text{LiAl}_{0.3}\text{Ti}_{1.7}(\text{PO}_4)_3$) [1,2]. These solid electrolytes are, however, difficult to sinter and their grain boundary resistance is generally very high. A second disadvantage is the presence of Ti^{4+} which is easily reduced to Ti^{3+} in contact with low-potential anodes (Li metal or C_6Li) and also limits the use of the material as a solid separator in contact with aqueous electrolytes. $\text{LiZr}_2(\text{PO}_4)_3$, alternatively, is expected to be electrochemically more stable than the titanium analog since Zr^{4+} is a stable oxidation state in materials with related structure. However, $\text{LiZr}_2(\text{PO}_4)_3$ exhibits very low ionic conductivity at room-temperature ($\sim 10^{-8} \text{ Scm}^{-1}$) [3,4]. The material also exhibits a complex polymorphism [5-10]. $\text{LiZr}_2(\text{PO}_4)_3$ phases prepared at relatively low calcination temperature ($\sim 900 \text{ }^\circ\text{C}$), commonly denoted as β -type phases, are reported to be orthorhombic (β phase) above $300 \text{ }^\circ\text{C}$ and monoclinic (β' phase: $\beta\text{-Fe}_2(\text{SO}_4)_3$ -type structure) below this temperature [7-9]. $\text{LiZr}_2(\text{PO}_4)_3$ prepared at higher calcination temperatures ($\sim 1200 \text{ }^\circ\text{C}$), on the other hand, is rhombohedral ($\alpha\text{-LiZr}_2(\text{PO}_4)_3$) above a transition temperature varying in the range $30\text{-}60 \text{ }^\circ\text{C}$; below this temperature, including room temperature, $\text{LiZr}_2(\text{PO}_4)_3$ is monoclinic/triclinic (α' -

$\text{LiZr}_2(\text{PO}_4)_3$) [5-7,10-14]. The ionic conductivity of α' - $\text{LiZr}_2(\text{PO}_4)_3$ is $\sim 5 \times 10^{-8} \text{ Scm}^{-1}$ at 30°C , while the conductivity of α - $\text{LiZr}_2(\text{PO}_4)_3$ at the same temperature is $\sim 10^{-5} \text{ Scm}^{-1}$ as estimated from extrapolating high-temperature measurements [3,4]. Efforts have therefore been directed to stabilize (rhombohedral) α - $\text{LiZr}_2(\text{PO}_4)_3$ at room temperature via several approaches such as varying synthesis conditions (e.g. quenching [15]) and aliovalent doping [16-18]. Mixed phases such as lithium zirconium/titanium phosphate and lithium zirconium phosphate/arsenate have also been prepared [19,20]. In this report a room-temperature stable α - $\text{LiZr}_2(\text{PO}_4)_3$ phase is successfully prepared using a modified sol-gel approach, which has enabled structural and electrical characterization of the material at room temperature for the first time.

2. MATERIALS AND METHODS

A modified sol-gel procedure was employed to synthesize $\text{LiZr}_2(\text{PO}_4)_3$. Lithium acetate (99.95%), zirconium oxynitrate hydrate (99%) and lithium dihydrogen phosphate ($\geq 98.0\%$) were purchased from Aldrich and used as starting materials. The degree of hydration in zirconium oxynitrate was determined experimentally by thermogravimetric analysis. Stoichiometric amounts of lithium acetate and zirconium oxynitrate hydrate were first dissolved in hot dilute nitric acid solution (2-3 wt. %) and then mixed slowly with EDTA (dissolved in NH_3 solution) and solid citric acid; mole ratio of total metal ions to EDTA and to citrate = 1:1:2. Dilute NH_3 solution was used to adjust the pH value of the solution to a value > 7 . After addition of drops of H_2O_2 solution (Aldrich, 30 wt. %; H_2O_2 /zirconium-ions mole ratio is greater than 1), a stoichiometric amount of lithium dihydrogen phosphate was then added slowly with continuous stirring. The resulting clear solution was heated at $\sim 110^\circ\text{C}$ to produce a transparent gel, which was subsequently heated at 250°C to form a black solid precursor. The solid precursor was

ground and calcined in air at 550 °C for 24h to remove organic components. The obtained powder was then isostatically pressed into pellets at 150 MPa and calcined in air at 1200 °C for 6h. An alumina disc covered with a thick platinum sheet was used as a sample holder for the calcination step. The sintered pellets were then either crushed to be examined by X-ray powder diffraction (XRD) or directly used for conductivity measurements. We found that syntheses starting with ~ 5 wt. % deficiency of the phosphate source (lithium dihydrogen phosphate) produce α -LiZr₂(PO₄)₃ phases of high purity.

X-ray diffraction (XRD) data were collected with an X'Pert Pro PANalytical (reflection mode) and a Bruker D8 (transmission mode) diffractometers, using CuK α radiations. Rietveld refinement based on XRD data were performed using the GSAS suite of programs [21]. Scanning electron microscopy (SEM) studies were performed using a MERLIN machine from Zeiss. AC impedance measurements were recorded using Alpha-A high performance modular measurement System (from Novocontrol technologies) in the frequency range of 10 MHz to 1 Hz and using an electrical perturbation of 20 mV. The data obtained were then analyzed by the software package WinDETA. Pellets with a thickness of 5–9 mm and a diameter of 10–13 mm were used in the conductivity measurements. Au electrodes were gas phase deposited on the circular sides of the pellets by thermal evaporation and copper discs were used to collect the current. Variable temperature conductivity measurements were carried out using a Novocool cryosystem (from Novocontrol technologies) in the temperature range –20 – 100 °C. Prior to each impedance measurement, the samples were equilibrated for 1 h at constant temperature. The differential scanning calorimetry (DSC) measurement was performed using a Seiko DSC 220 at a heating rate of 5 °C/min

3. RESULTS AND DISCUSSION

XRD analysis of the as-prepared $\text{LiZr}_2(\text{PO}_4)_3$ showed that the material is single-phase with no evidence of impurity or unreacted phases (Figure 2a). The XRD pattern of the material was readily indexed on a rhombohedral unit cell ($R\bar{3}c$ space group), consistent with a NASICON-type structure. The XRD pattern is characterized by the absence of the peak splitting which is commonly observed in previous studies and suggests a distortion of the NASICON-type structure [8,15,22]. No significant change is observed in the XRD pattern after storing the material for about one year (Figure 2b; the inset), indicating that no relaxation of the framework from rhombohedral to monoclinic/triclinic has occurred. Rietveld refinement based on XRD data of $\text{LiZr}_2(\text{PO}_4)_3$ was performed using the GSAS suite of programs. The crystal structure was refined by starting from the ideal NASICON atomic coordinates with Zr, P and O atoms in the (12c), (18e) and (36f) Wyckoff positions, respectively, of the $R\bar{3}c$ space group. Li was assumed to occupy the M1 site [i.e. the (6b) position]. This refinement led to a good agreement between the experimental and calculated patterns (Figure 2b) and to low reliability factors ($wRp = 0.0422$, $Rp = 0.0314$, $\chi^2 = 2.103$). However, due to the low sensibility of the refinement to the occupancy of the Li ion sites, the suggested Li ion positions remain an assumption. The refined unit cell parameters are $a = 8.85196(4) \text{ \AA}$ and $c = 22.1510(1) \text{ \AA}$. Interestingly, these parameters are very close to those reported for $\alpha\text{-LiZr}_2(\text{PO}_4)_3$ that is prepared by solid state reactions (at $1200 \text{ }^\circ\text{C}$) and stabilized at $150 \text{ }^\circ\text{C}$ ($a = 8.85493(3) \text{ \AA}$ and $c = 22.1440(1) \text{ \AA}$ [13]). In earlier reports [5,6], $\text{LiZr}_2(\text{PO}_4)_3$ is synthesized by the hydrolysis of an alcoholic solution containing zirconium alkoxide by using an aqueous solution containing lithium and phosphate ions; this procedure produces a monoclinic/triclinic $\text{LiZr}_2(\text{PO}_4)_3$ phase that converts to rhombohedral $\text{LiZr}_2(\text{PO}_4)_3$ (with $a \approx 8.85 \text{ \AA}$ and $c \approx 22.24 \text{ \AA}$) above a transition temperature varying in the

range 30-60 °C. Alamo et al. prepared $\text{LiZr}_2(\text{PO}_4)_3$ by dissolving reactants in acidic medium and claimed that the resulting phase is rhombohedral (with slight distortion) at room temperature, but they reported significantly different lattice parameters ($a \approx 8.79 \text{ \AA}$ and $c \approx 22.78 \text{ \AA}$) [15,22]. Hence, the $\alpha\text{-LiZr}_2(\text{PO}_4)_3$ phase prepared in this study has similar lattice parameters to that stabilized at temperatures above room-temperature, indicating that the transition temperature of $\text{LiZr}_2(\text{PO}_4)_3$ has probably been lowered to a value below room temperature.

Similar to $\text{LiTi}_2(\text{PO}_4)_3$ and other NASICON-type phases, the as-prepared $\alpha\text{-LiZr}_2(\text{PO}_4)_3$ phase showed low sinterability. The as-prepared pellets showed relatively low densities of about 74-77 % of the theoretical densities. Figure 3 shows the surface microstructure of the as-prepared $\alpha\text{-LiZr}_2(\text{PO}_4)_3$ pellet. The grains are in good contact with each other although a large amount of pores can be observed.

The ionic conductivity of the as-prepared $\alpha\text{-LiZr}_2(\text{PO}_4)_3$ was examined by AC impedance spectroscopy using gas-deposited gold electrodes. The impedance of the material shows a strong dependence on temperature. The impedance spectra can be described in terms of two semicircles (at high and intermediate frequencies) and a low frequency tail; and, over the studied frequency range, a shift of the observation window from left to right, i.e. towards lower frequencies, occurs as the temperature increases. Figures 4 and S1 (supporting information) show the Nyquist impedance plots for the material (two different pellets) in a temperature range from -20 to -100 °C. The high frequency semicircle disappears from the spectra at temperatures $> 30 \text{ °C}$. However, this semicircle progressively appears, and the low frequency spike diminishes, as the temperature is decreased (Figure 5). The impedance data were well fitted using $\text{R}(\text{RQ})(\text{Q})$, $\text{R}_e(\text{RQ})(\text{RQ})(\text{Q})$ or $\text{R}_e(\text{RQ})(\text{RQ})$ equivalent circuits depending on the temperature; (RQ) [a parallel resistance/constant-phase-element] and (Q) [a constant phase element] correspond to a

semicircle and the long tail in the z plane, respectively, while R_e is added to account for the electronic resistance of the measurement system. The impedance at 25 °C, for example, is fitted using the $R_e(RQ)(RQ)(Q)$ equivalent circuit (Figure 4d). Although the high frequency semicircle is not fully defined in this plot (Figure 5), the data were well fitted using $R_e(RQ)(RQ)(Q)$ rather than the $R(RQ)(Q)$ equivalent circuit. We generally attribute the first semicircle (high frequency), the second semicircle (intermediate frequency) and the low frequency tail to the impedance representing bulk, grain-boundary and electrode contributions, respectively. This is consistent with the results reported elsewhere where, within a fixed frequency range, the grain and grain boundary contributions to the impedance become more distinguishable, and the electrode contributions diminish, as the temperature decreases. This impedance behavior is also consistent with the behavior observed for isostructural $\text{LiTi}_2(\text{PO}_4)_3$ [23]. For $\text{LiTi}_2(\text{PO}_4)_3$ (and using lithium borate as a sintering aid), the semicircles corresponding to bulk and grain-boundary effects were observed at -50 °C while both disappeared at 90 °C. Since Au blocking electrodes are used in our experiments, the appearance of the low frequency tail (at appropriate temperatures) generally suggests that the observed transport effect is mainly ionic and corresponds to lithium ion mobility [24,25]. The bulk conductivities of the material could be therefore estimated from the fitting data of the high frequency semicircle, or the intercept of the intermediate frequency semicircle (at the high frequency side) with the real Z axis (for data collected at temperatures > 25 °C and fitted using $R(RQ)(Q)$ equivalent circuit).

The measured total and bulk conductivities of as-prepared $\alpha\text{-LiZr}_2(\text{PO}_4)_3$ at room temperature (25 °C) are 1.63×10^{-6} and $1.58 \times 10^{-4} \text{ Scm}^{-1}$, respectively. Another two different pellets showed total conductivities of 1.50×10^{-6} and $1.34 \times 10^{-6} \text{ Scm}^{-1}$. These values are close to those reported for $\text{LiTi}_2(\text{PO}_4)_3$ (total conductivity $2.0 \times 10^{-6} \text{ Scm}^{-1}$) which is isostructural to $\alpha\text{-LiZr}_2(\text{PO}_4)_3$ and

shows a similar morphology (lack of sinterability; $\sim 34\%$ porosity [2,26]). However, due to the absence of electrochemically active Ti^{4+} , a $\text{LiZr}_2(\text{PO}_4)_3$ -based membrane probably shows better characteristics as a solid electrolyte in all-solid-state batteries or as a solid separator between different liquid electrolytes contacting the anode and cathode. Goodenough et al. [16] reported total and bulk conductivities of Ca-doped $\text{LiZr}_2(\text{PO}_4)_3$ as $4.9 \times 10^{-5} \text{ Scm}^{-1}$ and $1.2 \times 10^{-4} \text{ Scm}^{-1}$, respectively. The bulk conductivity of $\text{Li}_{1.2}\text{Zr}_{1.9}\text{Ca}_{0.1}(\text{PO}_4)_3$ is similar to that observed for α - $\text{LiZr}_2(\text{PO}_4)_3$ in this study, however, the improved total conductivity is probably related to an improved sinterability due to Ca-doping. Hence, our study provides structural and conductivity data for α - $\text{LiZr}_2(\text{PO}_4)_3$ at room temperature that can be compared to the available data for isostructural phases such as $\text{LiTi}_2(\text{PO}_4)_3$, and also provide a base line for the ongoing attempts to stabilize and improve the sinterability of α - $\text{LiZr}_2(\text{PO}_4)_3$ by different approaches such as aliovalent doping.

The activation energy E_a for the Li-ion conduction of the material is obtained from the Arrhenius plot of $\sigma = \sigma_0 \exp(-E_a/kT)$, where σ_0 is the pre-exponential factor, k is the Boltzmann constant, T is the absolute temperature. The Arrhenius plots using the total and bulk ionic conductivities of α - $\text{LiZr}_2(\text{PO}_4)_3$ are shown in Figure 6a and the corresponding inset, respectively. The plots clearly show an inflection point at 16–18 °C indicating a change in the Li ion mobility in the material. This is attributed to a phase transition from rhombohedral to monoclinic/triclinic $\text{LiZr}_2(\text{PO}_4)_3$. The observed activation energies for the total conductivity before and after the transition are 0.39 and 0.99 eV respectively. Boilot et al. reported a similar slope discontinuity in the conductivity data of $\text{LiZr}_2(\text{PO}_4)_3$ at ~ 40 °C with activation energies 0.42 and 0.65 eV before and after the transition, respectively; however, different temperature ranges were used in their study [8]. The observed activation energy in our study, in the

temperature range $\sim 20 - 100$ °C, is slightly lower than that observed by Boilot et al. for $\text{LiZr}_2(\text{PO}_4)_3$ [8] and by Goodenough et al. for $\text{Li}_{1.2}\text{Zr}_{1.9}\text{Ca}_{0.1}(\text{PO}_4)_3$ [16,17]. The variable-temperature conductivity data of $\text{LiZr}_2(\text{PO}_4)_3$ are consistent with the DSC data recorded from material in the temperature range $-10 - 50$ °C (Figure 6b). An endothermic peak at ~ 15 °C is observed in the DSC curve of the material indicating that the as-prepared $\text{LiZr}_2(\text{PO}_4)_3$ exhibits $\alpha \rightarrow \alpha'$ transition below room temperature. Previous reports suggest that the $\alpha \rightarrow \alpha'$ transition in $\text{LiZr}_2(\text{PO}_4)_3$ occurs at temperatures varying in the range $30-60$ °C depending on the synthetic method. The synthesis method employed in this study, however, suggests that this limit can be stretched so that the transition temperature lies below room temperature which enables structural and electrical characterization of the material at room temperature. Several structural modifications related to the synthesis method may have occurred and probably account for the room temperature stability of rhombohedral $\text{LiZr}_2(\text{PO}_4)_3$, e.g. a deficiency of phosphate groups, incorporation of traces of carbonate groups or a disturbance of the Li ion distribution in the NASICON structure. We have recently observed a synthesis-related disturbance of Li ion distribution in $\text{LiTi}_2(\text{PO}_4)_3$ that led to modified structural and electrochemical properties of the NASICON-type material [27].

4. CONCLUSIONS

A modified sol-gel procedure that uses EDTA/citrate as complexing agent and employs a slight deficiency of the phosphate is successfully used to produce a room-temperature stable α - $\text{LiZr}_2(\text{PO}_4)_3$ phase. The as-prepared material undergoes no phase change upon storing for more than one year. The refined unit cell parameters are similar to those reported for α - $\text{LiZr}_2(\text{PO}_4)_3$ prepared by solid state reactions and stabilized at 150 °C. The measured total and bulk

conductivities of as prepared α -LiZr₂(PO₄)₃ at room temperature (25 °C) are $\sim 1.5 \times 10^{-6}$ and 1.5×10^{-4} Scm⁻¹, respectively. The estimated bulk conductivity is comparable to those reported for LiTi₂(PO₄)₃ and Li_{1.2}Zr_{1.9}Ca_{0.1}(PO₄)₃. The material undergoes phase transition to the α' -phase below room temperature (at ~ 16 – 18 °C). The activation energies for the total conductivity before and after the transition are 0.39 and 0.99 eV, respectively (in a temperature range -20 – 100 °C).

ACKNOWLEDGMENT

The authors acknowledge support by the Humboldt foundation (H. E.-S.), the LOEWE project STORE-E and the LaMa (Laboratory of Materials Research) at Justus-Liebig University (State of Hessen).

REFERENCES

1. H. Aono, E. Sugimoto, Y. Sadaoka, N. Imanaka, G.Y. Adachi, *J. Electrochem. Soc.* 136 (1989) 590–591.
2. H. Aono, E. Sugimoto, Y. Sadaoka, N. Imanaka, G. Adachi, *J. Electrochem. Soc.* 137 (1990) 1023–1027.
3. J. Kuwano, N. Sato, M. Kato, K. Takano, *Solid State Ionics* 70 (1994) 332–336.
4. K. Nomura, S. Ikeda, K. Ito, H. Einaga, *Solid State Ionics* 61 (1993) 293–301.
5. D. Petit, Ph. Colomban, G. Collin, J. P. Boilot, *Mat. Res. Bull.* 21 (1986) 365–371.
6. D. Petit, B. Sapoval, *Solid State Ionics* 21 (1986) 293–304.
7. M. Casciola, U. Costantino, L. Merlini, I. G. Krogh Andersen, E. Krogh Andersen, *Solid State Ionics* 26 (1988) 229–235.
8. F. Sudreau, D. Petit, J. P. Boilot, *J. Solid State Chem.* 83 (1989) 78–90.
9. M. Catti, N. Morgante, R. M. Ibberson, *J. Solid State Chem.* 152 (2000) 340–347.
10. K. Arbi, M. Ayadi-Trabelsi, J. Sanz, *J. Mater. Chem.* 12 (2002) 2985–2990.
11. J. E. Iglesias, C. Pecharrromán, *Solid State Ionics* 112 (1998) 309–318.
12. M. Catti, S. Stramare, R. Ibberson, *Solid State Ionics* 123 (1999) 173–180.
13. M. Catti, S. Stramare, *Solid State Ionics* 136 (2000) 489–494.
14. M. Catti, A. Comotti, S. Di Blas, *Chem. Mater.* 15 (2003) 1628–1632.

15. J. Sanz, J. M. Rojo, R. Jiménez, J. E. Iglesias, J. Alamo, *Solid State Ionics* 62 (1993) 287–292.
16. H. Xie, J. B. Goodenough, Y. Li, *J. Power Sources* 196 (2011) 7760–7762.
17. H. Xie, Y. Li, J. B. Goodenough, *RSC Advances* 1 (2011) 1728–1731.
18. Y. Li, M. Liu, K. Liu, C-A. Wang, *J. Power Sources* 240 (2013) 50–53.
19. A. Venkateswara Rao, V. Veeraiah, A.V. Prasada Rao, B. Kishore Babu, K.Vijaya Kumar, *Ceram. Int.* 40 (2014) 13911–13916.
20. V. I. Petkov, M. V. Sukhanov, A. S. Shipilov, V. S. Kurazhkovskaya, E. Yu. Borovikova, I. Yu. Pinus, A. B. Yaroslavtsev, *Inorg. Mater.* 50 (2014) 263-272.
21. A. C. Larson, R. B. Von Dreele, *General Structural Analysis System*, Los Alamos National Laboratory, Los Alamos, NM, 1994.
22. J. Alamo, J. L. Rodrigo, *Solid State Ionics* 32 (1989) 70–76.
23. H. Aono, E. Sugimoto, Y. Sadaoka, N. Imanaka, G.-y. Adachi, *Solid State Ionics* 47 (1991) 257–264.
24. V. Thangadurai, R. A. Huggins, W. Weppner, *J. Power Sources* 108 (2002) 64–69;
25. J. T. S. Irvine, D. C. Sinclair, A. R. West, *Adv. Mater.* 2 (1990) 132–138.
26. G.-y. Adachi, N. Imanaka, H. Aono, *Adv. Mater.* 8 (1996) 127–135.
27. H. El-Shinawi, J. Janek, *RSC Advances* 2015, DOI: 10.1039/C4RA16155F.

Figure captions

Figure 1. Part of the NASICON-type crystal structure showing the M1 and M2 crystal sites.

Figure 2. (a) XRD pattern of as-prepared α -LiZr₂(PO₄)₃. (b) Observed (+), calculated and difference profiles (solid lines) for XRD data collected from α -LiZr₂(PO₄)₃ ($\lambda=1.5406$ Å; wRp = 0.0422, Rp = 0.0314, $\chi^2 = 2.103$); the inset shows a part of the XRD pattern of α -LiZr₂(PO₄)₃ after storing the material for about one year.

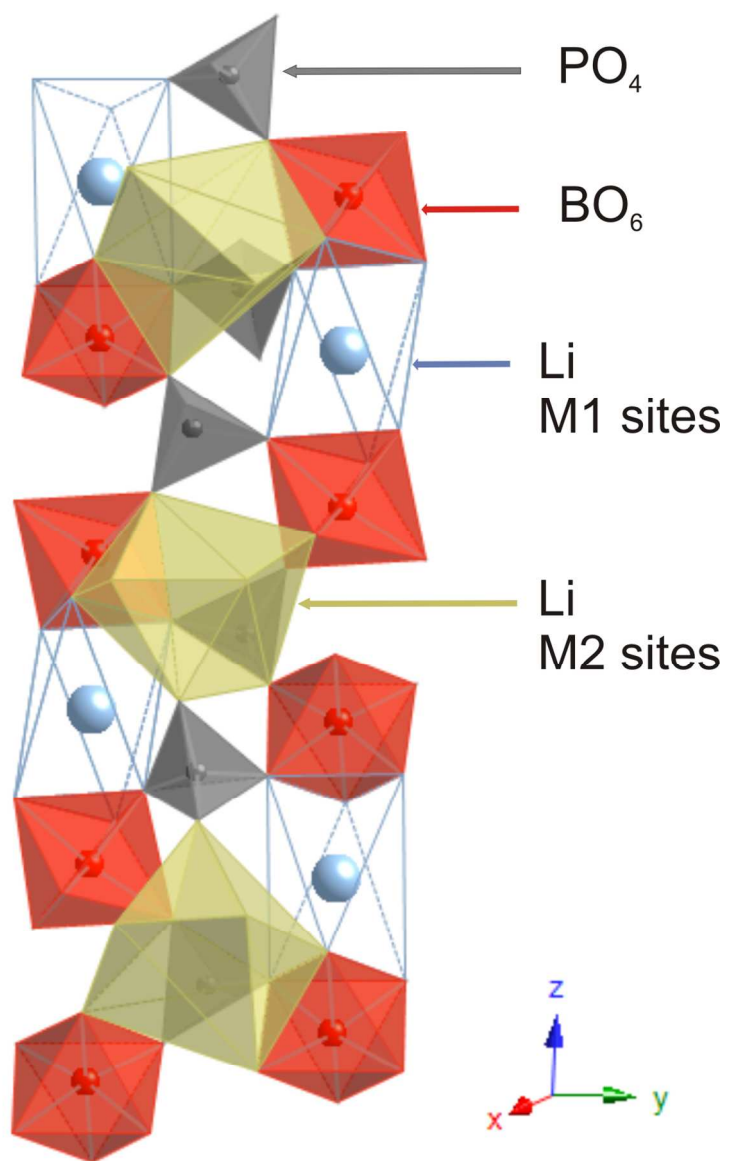
Figure 3. Surface microstructure of a sintered pellet of α -LiZr₂(PO₄)₃.

Figure 4. (a-c) Impedance spectra for α -LiZr₂(PO₄)₃ measured using Au electrodes (frequency range from 10 MHz to 1 Hz; 20 mV amplitude) in the temperature range -20 – 100 °C. (d) An equivalent circuit of the type R_e(RQ)(RQ)(Q); in the circuit, R is for resistance, Q for constant phase element and R_e for the electronic resistance of the measurement system; subscripts b, g and el refer to bulk, grain boundary and the blocking electrode, respectively.

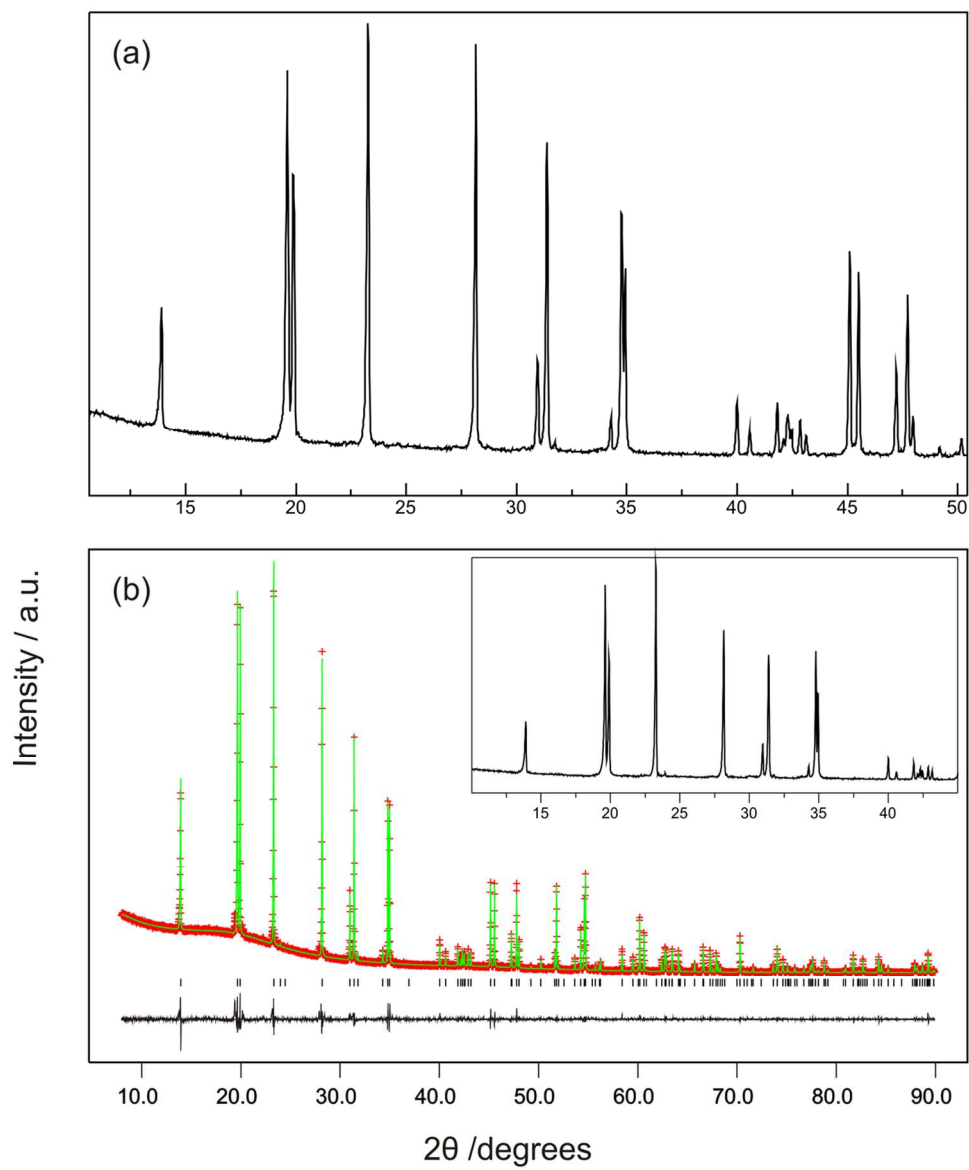
Figure 5. Impedance spectra for α -LiZr₂(PO₄)₃ measured at 25, 5, -10 and -20 °C, and fitted using the equivalent circuit R_e(RQ)(RQ)(Q) (25 °C) or R_e(RQ)(RQ) (5, -10 and -20 °C). The insets show zoom views of the plots in the frequency range 10 MHz to 0.1 MHz.

Figure 6. (a) Arrhenius plots for the total and bulk (inset) ionic conductivities of α -LiZr₂(PO₄)₃. (b) The DSC curve of LiZr₂(PO₄)₃ recorded during a heating treatment.

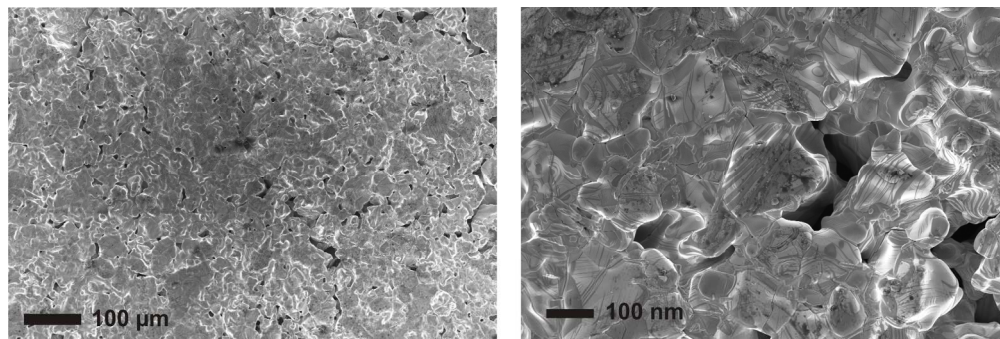
Figure S1. Impedance spectra for α -LiZr₂(PO₄)₃ measured using Au electrodes (frequency range from 10 MHz to 1 Hz; 20 mV amplitude) in the temperature range -20 – 110 °C.



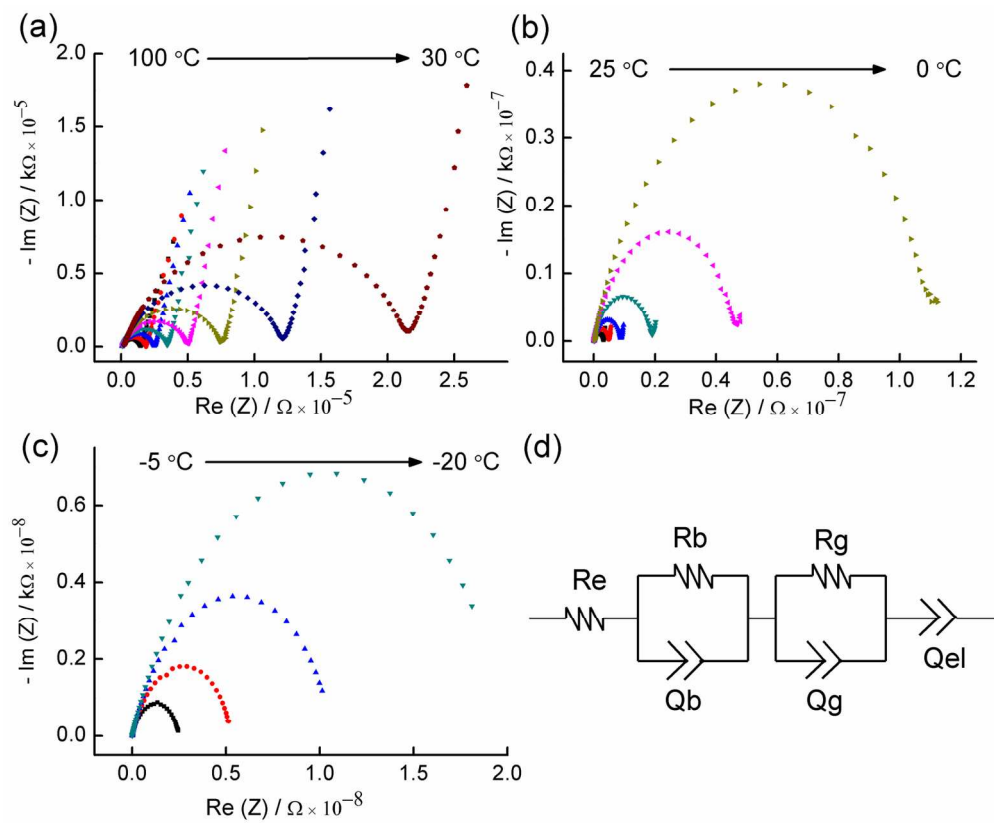
96x154mm (300 x 300 DPI)



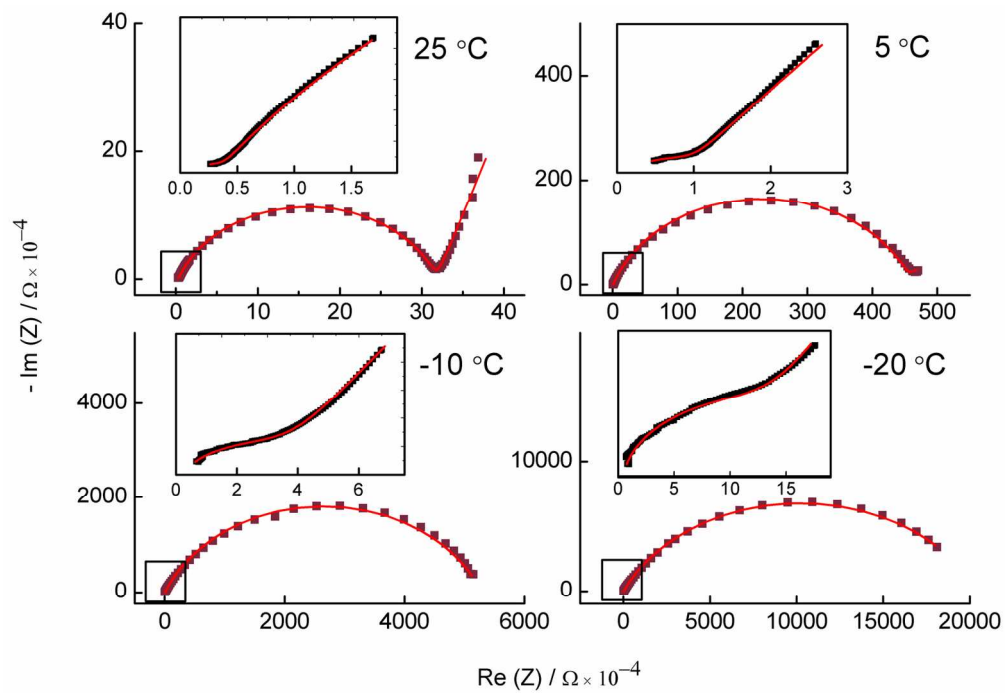
112x140mm (300 x 300 DPI)



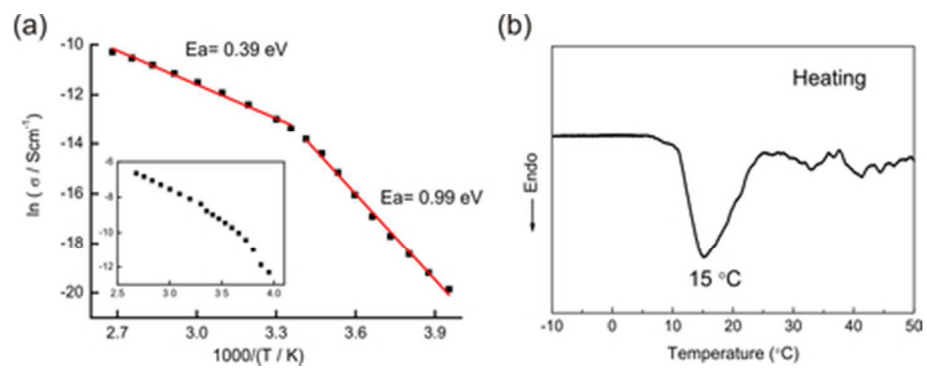
199x67mm (300 x 300 DPI)



149x122mm (300 x 300 DPI)



149x103mm (300 x 300 DPI)



38x14mm (300 x 300 DPI)

A table of contents entry

A room-temperature stable α -LiZr₂(PO₄)₃ phase is prepared by a modified sol-gel method, and shows bulk conductivity as high as $1.58 \times 10^{-4} \text{ Scm}^{-1}$.

